1   Research Article

2

3   **Ecological causes of speciation and species richness in the mammal tree of life**

4   Short title: Ecological causes of mammal diversity

5

6   **Nathan S. Upham[1*], Jacob A. Esselstyn[2], and Walter Jetz[3]**

7

8   Author affiliations:

9   [1]Department of Ecology & Evolutionary Biology, Yale University, New Haven, CT 06511 USA,

10   nathan.upham@yale.edu. [2]Department of Biological Sciences and Museum of Natural Science,

11   Louisiana State University, Baton Rouge, LA 70803 USA, esselstyn@lsu.edu. [3]Department of

12   Ecology & Evolutionary Biology, Yale University, New Haven, CT 06511 USA,

13   walter.jetz@yale.edu.

14

15   *Corresponding author:

16   165 Prospect St., OML 122, New Haven, CT 06511 USA, nathan.upham@yale.edu.

17

18

19

20

21

22

23

24

25

26

27

30

31   Abstract: 150 words; Main text: 4,620 words; 88 references, 5 figures

ABSTRACT

Biodiversity is distributed unevenly from the poles to the equator, and among branches of the tree of life, yet how those patterns are related is unclear. We investigated global speciation-rate variation across crown Mammalia using a novel time-scaled phylogeny (N=5,911 species, ~70% with DNA), finding that trait- and latitude-associated speciation has caused uneven species richness among groups. We identify 24 branch-specific shifts in net diversification rates linked to ecological traits. Using time-slices to define clades, we show that speciation rates are a stronger predictor of clade richness than age. Mammals that are low dispersal or diurnal diversify the fastest, indicating roles for geographic and ecological speciation, respectively. Speciation is slower in tropical than extra-tropical lineages, consistent with evidence that longer tropical species durations underpin the latitudinal diversity gradient. These findings juxtapose modes of lineage diversification that are alternatively turnover-based, and thus non-adaptive, or persistence-based as associated with resource adaptations.

INTRODUCTION

Biological diversity is concentrated at the equator more than the poles, and in some evolutionary lineages more than others. Yet how these organic phenomena are connected is an open question. The latitudinal diversity gradient is generally attributed to stable tropical productivity (*1–5*), but there is far less consensus regarding why species richness is distributed unevenly across the tree of life. Phylogenetic tree shape was first characterized taxonomically as species-per-genus 'hollow curves' (*6*) and later formalized under the concept of tree imbalance or unevenness (*7*). To arise, more speciose clades must have been derived from faster rates of net diversification (speciation – extinction), older ages (earlier divergences), or both. However, the relative contribution of clade rates and ages to species richness is widely disputed (e.g., (*8–11*)). Similarly controversial are the causes of diversification-rate variation in real phylogenies, whether due to stochasticity, determinism via ecological factors or time, or artifacts from how we reconstruct evolutionary history (*12–21*). Latitude might determine the rates at which new species originate and persist or go extinct (*2, 3, 22, 23*), but so too might species' intrinsic traits (*24*), some of which are correlated with latitude (e.g., (*25*)). Thus, understanding the causal underpinnings of uneven species richness patterns requires connecting levels of indirect (e.g., eco-geography) and direct (e.g., rates, ages) causes to assess their joint influences. Furthermore, investigating rate variation across large swaths of the tree of life simultaneously avoids ascertainment biases and methodological differences in compendia of smaller trees (*26*).

The last ~180-million-years of crown mammalian evolution have resulted in ~6000 living species (*27, 28*), which inhabit nearly all terrestrial biomes plus the open oceans, and thousands of preserved ancestors described as fossil taxa (*29–31*). Within this context, similarly aged clades in the mammal tree range from mega-diverse rodents (~2500 living species) and bats (~1300 species) to species-poor groups like treeshrews (20 species) and pangolins (8 species; all four share stem ages of ~60-70 million years ago [Ma] (*28, 32*)). The early availability of a species-level 'supertree' phylogeny of mammals (now cited over 1,800 times; (*33*)) encouraged initial studies of macroevolutionary-rate covariates (e.g., (*19, 34–36*)). However, because that pioneering supertree was assembled from hundreds of overlapping source trees, over 50% of its nodes were initially unresolved and then simulated to obtain a bifurcating time-scaled phylogeny (*33, 37*). Timings of diversification from this supertree, along with two other mammal supertrees

3

75 (*11*, *38*), were consequently shown to have inflated precision relative to the large gaps in

76 available fossil age and DNA sequence data (*28*).

77 Here, we draw upon a new species-level, time-calibrated phylogeny for global

78 Mammalia, which is built from a contiguous DNA supermatrix (31 genes by 4,098 species) and

79 consists of credible sets of 10,000 trees (*28*). We used these phylogenies, which jointly model

80 topological and age uncertainty, to better understand the temporal dynamics of mammalian

81 diversification relative to the potentially causal effects of organismal and environmental factors.

82 Our objectives were three-fold. We first tested for tree-wide and branch-specific rate variation in

83 relation to geological events such as the Cretaceous-Paleogene (K-Pg) mass extinction to explore

84 whether significant shifts in net diversification rates were mutually triggered. We then use

85 neutrally defined (time-slice based) clades to explore the relative roles of clade ages and

86 speciation rates in explaining current-day species richness. Finally, we develop the link between

87 observed variation in speciation rates and its putative ecological causes, testing whether factors

88 predicted to cause newly formed species to persist or go extinct are, in turn, causing the observed

89 patterns of uneven species richness.

90 We focus on three potential ecological causes (vagility, latitude, and diurnality) of rate

91 variation. First, we tested whether low-vagility species have higher speciation rates than more

92 dispersive species, due to their greater capacity to form nascent allopatric species (*39*, *40*). For

93 this test, we developed an index of organismal vagility for all mammals (i.e., dispersal ability;

94 (*41*)). Vagility has never been assessed across mammals, although evidence in birds using the

95 hand-wing index supports an inverse vagility-to-speciation rate relationship (e.g., (*42*, *43*)).

96 Second, if unstable environments increase species ephemerality via greater lineage turnover (*44*),

97 then we expect to find higher rates of recent species-specific (i.e., 'tip') speciation in temperate

98 latitudes where climates were historically less stable (*23*, *45*). To our knowledge, no latitudinal

99 tests of tip rates have been conducted in mammals to date, but clade-level comparisons have

100 either been inconclusive (*46*) or tentatively supported greater temperate than tropical lineage

101 turnover (*22*, *36*, *47*). Lastly, we test whether diurnality (daytime activity) has increased

102 speciation rates relative to nocturnal clades, following recent evidence that all mammals were

103 nocturnal until daytime niches evolved ~35 Ma (*48*, *49*). The influence of diurnality on

104 speciation rates has thus far only been investigated in primates (*50*), although a mammal-wide

105 study did investigate ancestral activity states (*49*). We are thus using species-level trait proxies to

106   investigate scenarios of geographic, ephemeral, and adaptive modes of species diversification in

107   mammals, respectively.

108   Overall, our approach ties together among-clade variation in rates, ages, richness, and

109   traits using phylogenetic path analyses, to our knowledge for the first time in any taxon. By

110   jointly assessing the causal contributions of ecological factors to the inferred tempo of

111   mammalian lineage diversification, we are able to elucidate their relative importance to

112   generating uneven species richness patterns. We uncover that vagility and diurnality are greater

113   causes of recent speciation-rate variation than latitude, with rate variation in turn contributing

114   more to uneven species richness than differences in clade age.

115

116   **RESULTS AND DISCUSSION**

117   **Tree-wide lineage diversification relative to the K-Pg event.** The Mammalia tree

118   shows substantial unevenness in species richness across major named clades (Fig 1a). We first

119   evaluated evidence for whether early placentals diverged before, after, or during the K-Pg event,

120   known as the short fuse, long fuse, and explosive models, respectively (*51*). The first four

121   placental divergences unambiguously preceded the K-Pg (Fig. 2a; filled circles), followed by the

122   next 21 divergences with CIs that overlap it (Fig. 2a–b). Therefore, we detect a Cretaceous

123   "fuse" of ~25-Ma between the radiation of crown Placentalia and nine of 18 crown orders (Fig.

124   2b), in line with some estimates (*32*, *52*), but longer than others (e.g., (*33*)).

125   Modeling branch-specific rates across the tree shows a pulse in both speciation and

126   extinction near the K-Pg (Fig. 2c) that remarkably matches concurrent fossil evidence for

127   increases in origination and extinction (Fig. 2d; synthesized from the Paleobiology Database

128   (*30*)), as well as tree-wide shifts to higher net diversification rates in the 5-Ma following the K-

129   Pg (Fig. S5-S7). Such dynamics of lineage turnover following the K-Pg are previously reported

130   in fossil eutherians (*51*, *53*), as attributed to selective extinction followed by ecological

131   opportunity for the surviving mammal lineages (*54*, *55*). Thus, this fossil-calibrated molecular

132   phylogeny (*28*) appears to reflect dynamics evident from the fossil record alone.

133   **Branch-specific rate shifts relative to time and traits.** We recover shifts in net

134   diversification rates at 24 consistent locations in the mammal tree (Fig. 1a, 2c, e; shifts are

135   present in ≥ 50% of maximum shift credibility trees using BAMM (*56*), see *Supplementary*

136   *Materials* Fig. S7, Table S1). The earliest rate shift occurs in either crown Placentalia (1.1x

137 higher than the median background rate of 0.138 species/lineage/Ma) or Boreoeutheria (1.6x,

138 node C in Fig. 1a). These shifts involve 18 different lineages, 15 of which are consistent

139 increases. The only rate decrease was in the strepsirrhine primates (lemurs, lorises, and galagos;

140 node O). Two other shifts are alternately up or down, depending on the tree sampled (nodes H, P;

141 Fig. 1a). This result compares to 27 rate-shifted clades detected on the original mammal

142 supertree using an earlier method (15 increasing and 12 decreasing (*19*)—but note caveats about

143 the identifiability of downshifts (*57*)). Overall, rate increases nearer the present are higher, with a

144 2.2x mean in the Miocene versus 1.3x in each the Oligocene and Eocene (Fig. 2c; df=2, F=7.772,

145 P=0.003). This result is consistent with the expectation for extinctions deeper in the tree to have

146 reduced our ability to quantify more ancient shifts (*56, 58*), as well as fossil and molecular

147 evidence that younger clades tend to have faster rates of diversification (*21*).

148   Species in rate-shifted clades overall have dissimilar ecologies (Fig. 1b), yet share more

149 attributes than expected if idiosyncratic mechanisms were entirely fostering major radiations. We

150 note the conspicuous latitudinal pattern of alternating south-north-south endemism among major

151 rodent clades, which may relate to historical biogeographic incumbency (e.g., (*59*)). Strikingly,

152 the two largest rate increases (4.0x and 3.2x) occurred in lineages with disparate life modes but

153 similar propensities for genetic isolation: the fossorial tuco-tucos of South America (*Ctenomys*,

154 node Q), and the Indo-Pacific flying foxes (*Pteropus*, node J; Fig. 1a). Thus, small burrowers and

155 large flyers both show similar signatures of recent and rapid speciation under conditions of

156 insularity, although in subterranean and oceanic realms, respectively. Tree-wide tests of trait-

157 dependent speciation suggest that high vagility is marginally associated with novel rate regimes

158 (STRAPP (*60*) one-tailed test, P = 0.08), which is contrary to the inverse vagility-to-speciation

159 relationship we expected (*39, 40*). However, these tests are complicated by the fact that many

160 high-vagility lineages are also diurnal, and diurnality is a clearly associated with shifts to higher

161 speciation-rate regimes (P = 0.027; Fig. S8). Diurnality-associated rate shifts in simian primates,

162 carnivorans, cows, and whales (shifts N, D-F, and Q; Fig. 1a) also contain a majority of high-

163 vagility species (>1 km natal dispersal distance), and many with large latitudinal breadths (Fig.

164 1b). We thus highlight the need to tease apart the relative contributions of vagility, latitude, and

165 diurnality to understand their effects upon rate heterogeneity in mammalian clades.

166   **Named clade rate variation.** Beyond rate-shifted clades, we consider diversification-rate

167 variation within the five most speciose placental orders (Fig. 2e-f). Testing fits to diversification

168   models of rate-variable processes through time (RV, exponential or linear; (*61*)) versus rate-

169   constant ones (RC, single rates of birth or death), we find greater fits to RV models in five of the

170   12 named subclades examined (Fig. 2f; Table S2). The mouse-related clade of rodents (clade 20

171   in Figs. 1, 2f) has a branching pattern best fit by RV processes in all 100 trees examined, as

172   expected from the seven branch-specific rate shifts already uncovered in that clade (nodes R-X in

173   Figs. 1, 2). Shrews, catarrhine primates, and the cow- and whale-related clades of artiodactyls

174   join mice in showing greater RV fits than expected from RC simulation, as well as one rate shift

175   each (clades 6, 15, 10, and 11; Fig. 2f).

176   Since jump-shift processes were not directly compared to time-varying RV ones, or to

177   tree-wide shift scenarios (Fig. S5-S7), these models were not differentiable by our tests. In

178   theory, they may require considerably more fossil data to be identifiable (*62*). Nevertheless,

179   clade-specific fossil and molecular evidence supports our assertion that ancestral whales and

180   dolphins entered a novel macroevolutionary regime, including selection toward larger body sizes

181   (*56*, *60*, *61*, *63*). Bats, on the other hand, display an inconsistent fit to RV models of

182   diversification (clades 12-13, Fig. 2f), and an inconsistent number of rate shifts between our

183   study (six, nodes G-L, Fig. 1a) and a previous one (two, nodes H and J; (*64*)). We suggest that

184   high levels of topological uncertainty, which is arguably greater in bats than other orders (*65*), is

185   contributing to the equivocal modeling of RC, RV, and jump-shift processes across credible tree

186   sets for bats (Table S2).

187   As an additional, more sensitive, test of within-clade rate variation, we use clade-wide

188   distributions of tip-level speciation rates as assessed using the tip DR metric (*66*) (Fig. 2f).

189   Broadly, we recognize substantial heterogeneity in tip rates across the mammal tree, sometimes

190   with a few high-tip-rate species nested together with lower-rate species (Fig. 1a), resulting in

191   long right-side tails in the tip-rate distributions (positive skew, e.g., bat and rodent clades 12 and

192   18; Fig. 1a, 2f). We propose that tip rate skew measures aspects of within-clade speciation-rate

193   variation that is otherwise uncaptured by fitting *a priori* models of the diversification process

194   (Table S3), and thus offers a distinct predictor of among-clade variation in species richness.

195   **Time-slice clade richness relative to ages and rates.** The relative importance of clade

196   ages (time) versus rates of speciation and extinction (whether stochastic or ecologically

197   deterministic) as an explanation of extant diversity levels is widely debated (*8–12*, *16*, *17*).

198   Original claims that uneven trees are random outcomes of constant-rate diversification (e.g.,

199   (*67*)) have been refuted (*10*, *13*, *18*). However, past efforts to separate these hypotheses have

200   focused on named clades (e.g., (*10*)), which are biased by subjective delineation and often vast

201   age differences (mammal families range 3.8–59.0 Ma in mean crown ages; (*28*)).

202   To avoid problems associated with subjective clade definitions, we sliced phylogenies at

203   five-million-year intervals and took the tipward clades as objective units for analysis (Fig. 3).

204   Time-sliced clades thus account for the 'pull of the present' in modern trees (*58*) by analyzing

205   successive levels of rootward covariance among clade crown age, species richness, tip rate mean

206   and skew, and mean ecological traits. If time-constant rates predominate (*11*, *12*, *17*), crown ages

207   will explain the most among-clade variation in species richness. In contrast, if rate variation is

208   strong, as we already recognized for some nodes and named clades (Fig. 2) and expect from

209   varying ecological regimes (*7*, *19*, *39*, *68*), diversification rates will have the greater explanatory

210   power.

211   We find that clade age and richness are positively correlated—yet significantly less so

212   than the unique effects of tip rate mean and skew on richness (Fig. 4, multivariate PGLS; Fig.

213   S10 for univariate and taxon-based results). Critically, clade tip rate mean has stronger effects on

214   richness than expected from simulated birth-death trees containing only stochastic rate variation

215   (Fig. 4b). Clade tip rate skew is also significant, especially so at deeper time slices (Fig. 4c),

216   confirming that single speed-ups in diversification within a clade (e.g., due to a rate shift in one

217   lineage) can drive much of its overall species richness today. These analyses are robust to the

218   influence of species that are missing DNA sequences and imputed (Fig. S10). Our findings thus

219   support arguments that 'ecology' (broadly defined to include any extrinsic or intrinsic factor that

220   alters macroevolutionary-rate processes) is a greater cause of species richness variation than time

221   (*16*); however, both clearly contribute to observed richness (adjusted-R^2: 0.88 full model versus

222   0.74 with tip rate mean only and 0.26 with crown age only, means of 100-tree PGLS among 35-

223   Ma clades). Jointly analyzing richness determinants in time-sliced clades offers an objective way

224   to assess age and rate effects that, in turn, enables tests for which ecological factors are driving

225   that rate variation.

226   **Linking uneven rate variation to ecological factors.** We performed phylogenetic path

227   analysis (*69*) to assess the hypothesized effects of species vagility (*39*, *40*), latitude (*22*, *23*), and

228   diurnality (*48*) upon the joint, yet unequal, contributions of rates and ages to extant species

229   richness variation (Fig. 5, *Methods*, Fig. S4). Here, the time-sliced clades allow us to distinguish

230   trait-rate dynamics that are localized near the species level (if traits drive ephemeral speciation

231   (*44*) or if they evolved very recently) from those that occur deeper in the tree and persist (if traits

232   evolved anciently and did not affect extinction rates). Our assembly of species-level traits across

233   Mammalia (Fig. 1b) enables us to directly pass information to clade-level means, thereby

234   summarizing the ecological 'essence' of that clade for a given trait. However, we note that other

235   statistical moments (e.g., trait variance or skew) may prove useful for future study.

236   At the species level, we find that low-vagility mammals have higher tip speciation rates,

237   especially in herbivores and carnivores (Fig. 5a; ecological trait ~ rate PGLS (*70*)). Effects of

238   vagility on clade tip rate mean are weakened at deeper time slices, where they are instead

239   recorded on tip rate skew (Fig. 5b). We interpret these short-lived effects of vagility on

240   speciation rates as consistent with expectations that nascent allopatric species are produced at a

241   high rate, but are ephemeral, going extinct before they can expand their geographic range (*39,*

242   *40*, *44*, *71*). While the nearly 20% of mammal species that are endemic to islands complicates

243   our allometric vagility index, we note that the ~10-million-year 'threshold' whereby low-vagility

244   lineages find an adaptive zone, evolve greater vagility, or vanish is robust to multiple sensitivity

245   tests (Fig. S13-S14). The influence of vagility on mammal diversification, however, might be

246   non-linear as it is in birds (e.g., humped (*39*) or sigmoidal (*43*)).

247   To test the causal role of environmental stability in the generation of mammalian tree

248   shape (*3*, *23*, *45*), we evaluate the impact of latitudinal centroid distance from the equator upon

249   speciation rates. Contrary to the expectations of ephemeral speciation processes driving recent,

250   high rates of speciation at temperate latitudes (*22*, *23*, *45*), we find no effect of absolute latitude

251   on tip-level speciation (Fig. 5a). Instead, strong positive associations with latitude only arise at

252   deeper time slices, and without any corresponding effects on clade tip rate skew (Fig. 5b).

253   Similarly weak latitude-to-rate effects in young clades and species of birds (*22*, *45*, *66*, *72*)

254   appear to emphasize that species turnover cycles are erasing a portion of the latitudinal effect.

255   We suggest that the traditionally invoked tropical 'cradle' (higher speciation) and 'museum'

256   (lower extinction (*3*)) should re-focus upon the *combined turnover* of those processes and test

257   whether extratropical species are 'cycled' faster than tropical species. Extratropical lineages may

258   not cycle fully, but instead persist through climatic oscillations in glacial refugia (*73*). In that

259   case, the Eocene-Oligocene (~34 Ma) expansion of temperate habitats (*3*) may have initiated

260   converse latitudinal gradients in species turnover rates and total richness. Within North America,

9

261   the fossil record suggests the latitudinal gradient in mammalian richness was not established

262   until ~15 Ma (*74*).

263   Lastly, we queried the effect of diurnality, a core behavioral trait thought of as a temporal

264   niche innovation (*48*). We find that repeated origins of daytime activity since the late Eocene

265   (~35 Ma (*48*, *49*)) are associated with faster speciation, both at the present (Fig. 5a) and among

266   time-sliced clades at 10 Ma (Fig. 5b). These findings complement the signature of greater diurnal

267   activity on rate-shifted clades (Fig. S8), as well as place previous findings of rapid diversification

268   in diurnal lineages of primates (*50*) in a broader context. We suggest that inverse effects of

269   diurnality on tip rate skew at deeper time slices (Fig. 5b) are misleading given the evolution of

270   daytime activity ~35 Ma, well after a 'nocturnal bottleneck' among K-Pg-surviving mammals

271   (*48*, *49*). We posit that greater daytime activity is an example of an adaptive divergence in niche

272   traits that has decreased extinction rates via competitive release (i.e., an 'ecological opportunity';

273   (*68*, *75*)), and therefore led to greater species richness via persistence.

274

275   **CONCLUSION**

276   Our analyses here connect ecological factors to their time-scale-dependent effects on

277   speciation and diversification in mammals. We detect cross-clade signatures of intrinsic

278   (vagility, activity pattern) and extrinsic (latitude) factors driving aspects of lineage

279   diversification at nested phylogenetic levels. We hypothesize that two main processes are at

280   work. First, turnover-associated speciation is acting on short timescales due to geographic

281   isolation among low-vagility species, and on longer time scales, from the dynamics of

282   extratropical climates. Second, persistence-associated speciation is occurring in diurnal lineages

283   as an example of a trait that adaptively couples greater speciation with lower extinction rates.

284   Traversing from the first to second macroevolutionary mode may be possible if otherwise

285   ephemeral allopatric species enter novel regions of ecological space, either via niche evolution or

286   extrinsic opportunity, to then differentially persist under lower extinction risk (*44*, *68*, *71*, *75*).

287   Future tests that leverage direct measurements of fossil extinction rates in lineages that have

288   evolved low vagility or diurnality will be valuable for assessing the frequency of these

289   contrasting diversification modes.

290   Overall, we show that ecological factors influence speciation rates, but the effects

291   manifest at different hierarchical levels of the tree due to apparent differences in associated

10

292   lineage turnover. The longstanding gradient of greater tropical than temperate environmental

293   stability has led to longer species durations for tropical mammals. Geologically recent processes

294   associated with species turnover or adaptive persistence are not yet studied for most of life, but

295   our results for mammals suggest that lineage-level gradients in these novelty-originating

296   processes have causes that are rooted in the dynamics of population-level gene flow. Efforts to

297   connect evolutionary levels from individual organisms to speciose clades thus appear most

298   promising for understanding the causes and consequences of geographically and

299   phylogenetically uneven species richness across the broader tree of life.

300

301   **METHODS**

302   **Mammalian phylogeny and species trait data.** We leveraged the recently constructed

303   species-level mammal trees of Upham et al. (*28*) to conduct all analyses. Briefly, these

304   phylogenies include 5,804 extant and 107 recently extinct species in credible sets of 10,000 trees.

305   They are built using a 'backbone-and-patch' framework that used two stages of Bayesian

306   inference to integrate age and topological uncertainty, and incorporate 1,813 DNA-lacking

307   species using probabilistic constraints (available at vertlife.org/phylosubsets). We compared

308   credible sets of trees built using node-dated backbones (17 fossil calibrations) and tip-dated

309   backbones (matrix of modern and Mesozoic mammals), as well as taxonomically completed

310   trees (5911 species) versus trees of DNA-only species without topology constraints (4098

311   species).

312   Our workflow for gathering trait data involved (i) unifying multiple trait taxonomies

313   (e.g., EltonTraits v1.0 (*76*), PanTHERIA (*77*)) to our phylogeny's master taxonomy; and (ii)

314   interpolating home range area and vagility to the species level using known allometric

315   relationships in mammals (Fig. S2). Vagility was calculated as the maximum natal dispersal

316   distance per individual (km) and interpolated for each species following our updated version of

317   Whitmee and Orme's (*41*) best-fit equation, which applies species means of body mass, home

318   range, and geographic range (Fig. S3). Note that our vagility index does not account for

319   locomotor abilities (e.g., flying or arboreality), but rather captures aspects of space use that scale

320   allometrically across mammals.

321   **Tip-level speciation rates.** We calculated per-species estimates of expected pure-birth

322   diversification rates for the instantaneous present moment (tips of the tree) using the inverse of

323 the equal splits measure (*66, 78*). This metric has been called 'tip-level diversification rate' (tip

324 DR) because it measures recent diversification processes among extant species (*79*). However, to

325 avoid confusion with 'net diversification', for which tip DR is misleading when extinction is

326 very high (relative extinction >0.8 (*80*)), we here refer to tip DR as a tip-level speciation rate

327 metric. At the tip level, we show that tip DR is tightly associated with model-based estimators of

328 speciation and net diversification rates in our trees (Fig. S1a). At the clade-level, we measure

329 'clade tip speciation mean' as the harmonic mean of tip DR among species, which is known to

330 converge to the maximum likelihood estimator of pure-birth diversification rate in clades with

331 >10 species (*66, 78*). We show that clade tip DR mean indeed best approximates pure-birth clade

332 rates for time-sliced clades in our mammal trees (R^2: ~0.7 versus ~0.5 for birth-death speciation

333 and net diversification rates; Fig. S1b).

334   **Branch-specific and tree-wide rate shifts.** We performed searches for

335 macroevolutionary shifts using BAMM v2.5 (*56*), a reversible-jump algorithm for sampling

336 birth-death rate regimes without a prior hypothesis. We evaluated the number and location of

337 rate shifts on 10 trees from the node-dated sample of complete mammal trees. We summarized

338 across the most likely shifts per tree—called maximum shift credibility (MSC) sets (Fig. S7)—

339 using the ratio of the mean net diversification rate of all branches inside the shifted clade (clade

340 rate) and outside that clade (background rate) to calculate the rate shift magnitude and direction

341 for each MSC set (Table S1). For tree-wide rate shifts, we compared results from TreePar (*34*)

342 and CoMET (*81*) (see details in Fig. S5-S6).

343   **Comparisons with fossil genus diversification.** To assess the congruence of our

344 molecular phylogeny-based rate estimates with rates estimated from the fossil record, we

345 analyzed Mammalia fossil occurrence data from the Paleobiology Database (*30*). Grouping by

346 genus after excluding ichnotaxa and uncertain genera, we recovered 71,928 occurrences of 5300

347 genera, which we then binned in 10-Ma intervals (taxa spanning boundaries go in both bins) and

348 used shareholder quorum subsampling (SQS (*82*); quorum size: 0.5) to maximize the uniformity

349 of coverage. We then calculated corresponding origination and extinction rates per stage using

350 the per-capita rate method (*83*).

351   **Likelihood testing for models of diversification.** We analyzed the branching times of

352 27 named subclades (11 orders and 16 suborders) that contained ≥ 25 species. For each subclade,

353 we tested 10 models developed by Morlon et al. (*61*): two rate-constant (RC) models, constant

354 pure-birth and birth-death; and eight rate-variable (RV) models, with exponentially and linearly

355 time-varying rates. We fit models for 100 trees of the empirical subclades and their matching

356 RC-simulated trees (null models, simulated under the empirical extinction fractions of ~ε=0.65

357 over 100 trees using the "pbtree" function in phytools (*84*)). Subtracting AICc scores of the best-

358 fitting RC and RV models provided the ΔAIC_{RC-RV} test statistic (*85*) per tree and subclade for

359 comparison to the simulated null distribution (alpha=0.05; see Table S2).

360 **Time-sliced clades and clade-level tests of species richness variation.** To objectively

361 define clades, we arbitrarily drew lines (referred to as "time slices") at 5-Ma intervals and took

362 the resulting *tipward* (all the way to the extant tip) monophyletic clades as non-nested units of

363 analysis. The *rootward* relationships of those clades (the "rootward backbone") was retained for

364 each interval, giving the expected covariance structure among clades when performing

365 phylogenetic generalized least squares (PGLS) analyses (see Fig. 3 for illustration). We used the

366 "treeSlice" function in phytools to construct clade sets across Mammalia trees and the three sets

367 of RC simulations, empirical (ε=0.65), low (ε=0.2), and high (ε=0.8), also comparing our results

368 to analyses on traditional taxon-based clades (genera, families, and orders; Fig. S10-S12). All

369 PGLS was performed excluding extinct species, using Pagel's "lambda" transformation in

370 phylolm (optimized for large trees (*86*)), and repeating the analysis across 100 or 1000 trees. We

371 also performed multivariate analyses including percent of DNA-sampled species per clade to test

372 whether our results are unaffected by imputing DNA-missing species (Fig. S10).

373 **Tip-level tests of speciation-rate correlates.** To examine correlative structures

374 underlying observed tip-rate variation, we performed tip-level PGLS analyses between species'

375 ecological traits and tip DR values across 1000 trees, focusing on a 5675-species data set that

376 excluded all extinct (n=107) and marine (n=129) species. We followed Freckleton et al. (*70*) in

377 using trait ~ rate models in our tip-level PGLS analyses to avoid identical residuals in the

378 dependent variable (i.e., sister species have identical tip DR values, which otherwise violates the

379 assumed within-variable data independence in bivariate normal distributions). The trait ~ rate

380 approach was previously applied using tip DR in univariate contexts (*87*) (see Fig. S13-S14 for

381 sensitivity tests).

382 **Clade-level tests of speciation-rate correlates.** At the clade level, univariate PGLS was

383 performed typically (rate ~ trait models), since clade tip DR mean gave independent values to

384 sister clades. These analyses were conducted on 1000 trees by analogy with those previous,

13

385 except that per-clade trait summaries were standardized predictors (mean centered, standard

386 deviation scaled) using geometric means for vagility and arithmetic means otherwise. We also

387 performed tests for trait-dependent speciation using rate-shifted clades identified in BAMM runs

388 on 10 mammal trees (STRAPP (*60*) method), which corrects for phylogenetic pseudoreplication

389 similar to PGLS except instead via the covariance structure among rate regimes (see Fig. S8).

390   **Phylogenetic path analyses.** We performed path analysis aiming to fully resolve

391 correlational structures and thereby translate from the language of statistical association to

392 causality. For phylogenetic path analyses, we used PGLS to test statements of conditional

393 independence (*69*) across 27 pre-selected path models (Fig. S4). For each tree and clade set, we

394 used "phylopath" (*88*) to analyze models and perform conditional model averaging. Time-sliced

395 clades at 10-, 30-, and 50-Ma intervals were analyzed and compared to analogous results using

396 taxon-based clades (Fig. S12).

397

References

1. P. V. A. Fine, R. H. Ree, Evidence for a Time-Integrated Species-Area Effect on the Latitudinal Gradient in Tree Diversity. *Am. Nat.* **168**, 796–804 (2006).

2. D. Jablonski, K. Roy, J. W. Valentine, Out of the Tropics: Evolutionary dynamics of the latitudinal diversity gradient. *Science*. **314**, 102–106 (2006).

3. G. G. Mittelbach, D. W. Schemske, H. V. Cornell, A. P. Allen, J. M. Brown, M. B. Bush, S. P. Harrison, A. H. Hurlbert, N. Knowlton, H. A. Lessios, C. M. McCain, A. R. McCune, L. A. McDade, M. A. McPeek, T. J. Near, T. D. Price, R. E. Ricklefs, K. Roy, D. F. Sax, D. Schluter, J. M. Sobel, M. Turelli, Evolution and the latitudinal diversity gradient: speciation, extinction and biogeography. *Ecol. Lett.* **10**, 315–331 (2007).

4. W. Jetz, P. V. A. Fine, Global Gradients in Vertebrate Diversity Predicted by Historical Area-Productivity Dynamics and Contemporary Environment. *PLOS Biol.* **10**, e1001292 (2012).

5. R. Jansson, G. Rodríguez-Castañeda, L. E. Harding, What Can Multiple Phylogenies Say About the Latitudinal Diversity Gradient? A New Look at the Tropical Conservatism, Out of the Tropics, and Diversification Rate Hypotheses. *Evolution*. **67**, 1741–1755 (2013).

6. J. C. Willis, *Age and Area* (Cambridge University Press, Cambridge, 1922).

7. A. O. Mooers, S. B. Heard, Inferring Evolutionary Process from Phylogenetic Tree Shape. *Q. Rev. Biol.* **72**, 31–54 (1997).

8. M. A. McPeek, J. M. Brown, Clade age and not diversification rate explains species richness among animal taxa. *Am. Nat.* **169** (2007).

9. J. J. Wiens, The causes of species richness patterns across space, time, and clades and the role of "ecological limits". *Q. Rev. Biol.* **86**, 75–96 (2011).

10. D. L. Rabosky, G. J. Slater, M. E. Alfaro, Clade age and species richness are decoupled across the eukaryotic tree of life. *PLoS Biol.* **10**, e1001381 (2012).

11. S. B. Hedges, J. Marin, M. Suleski, M. Paymer, S. Kumar, Tree of life reveals clock-like speciation and diversification. *Mol. Biol. Evol.*, msv037 (2015).

12. R. E. Ricklefs, Global diversification rates of passerine birds. *Proc. R. Soc. Lond. B-Biol. Sci.* **270**, 2285–2291 (2003).

13. M. G. B. Blum, O. François, Which Random Processes Describe the Tree of Life? A Large-Scale Study of Phylogenetic Tree Imbalance. *Syst. Biol.* **55**, 685–691 (2006).

14. A. B. Phillimore, T. D. Price, Density-dependent cladogenesis in birds. *PLoS Biol.* **6**, e71 (2008).

15. D. L. Rabosky, Ecological limits and diversification rate: alternative paradigms to explain the variation in species richness among clades and regions. *Ecol. Lett.* **12**, 735–743 (2009).

16. T. D. Price, The roles of time and ecology in the continental radiation of the Old World leaf warblers (*Phylloscopus* and *Seicercus*). *Philos. Trans. R. Soc. Lond. B Biol. Sci.* **365**, 1749–1762 (2010).

17. C. Venditti, A. Meade, M. Pagel, Phylogenies reveal new interpretation of speciation and the Red Queen. *Nature*. **463**, 349–352 (2010).

18. T. J. Davies, A. P. Allen, L. Borda-de-Água, J. Regetz, C. J. Melián, Neutral Biodiversity Theory Can Explain the Imbalance of Phylogenetic Trees but Not the Tempo of Their Diversification. *Evolution*. **65**, 1841–1850 (2011).

19. A. Purvis, S. A. Fritz, J. Rodríguez, P. H. Harvey, R. Grenyer, The shape of mammalian phylogeny: patterns, processes and scales. *Philos. Trans. R. Soc. Lond. B Biol. Sci.* **366**, 2462–2477 (2011).

20. D. S. Moen, H. Morlon, Why does diversification slow down? *Trends Ecol. Evol.* **29**, 190–197 (2014).

21. L. F. H. Diaz, L. J. Harmon, M. T. C. Sugawara, E. T. Miller, M. W. Pennell, Macroevolutionary diversification rates show time dependency. *Proc. Natl. Acad. Sci.*, 201818058 (2019).

22. J. T. Weir, D. Schluter, The Latitudinal Gradient in Recent Speciation and Extinction Rates of Birds and Mammals. *Science.* **315**, 1574–1576 (2007).

23. A. D. Cutter, J. C. Gray, Ephemeral ecological speciation and the latitudinal biodiversity gradient. *Evolution.* **70**, 2171–2185 (2016).

24. D. Jablonski, Species Selection: Theory and Data. *Annu. Rev. Ecol. Evol. Syst.* **39**, 501–524 (2008).

25. J. Alroy, Small mammals have big tails in the tropics. *Glob. Ecol. Biogeogr.* **0** (2019), doi:10.1111/geb.12912.

26. J. M. Beaulieu, B. C. O'Meara, Can we build it? Yes we can, but should we use it? Assessing the quality and value of a very large phylogeny of campanulid angiosperms. *Am. J. Bot.* **105**, 417–432 (2018).

27. C. J. Burgin, J. P. Colella, P. L. Kahn, N. S. Upham, How many species of mammals are there? *J. Mammal.* **99**, 1–14 (2018).

28. N. S. Upham, J. A. Esselstyn, W. Jetz, Inferring the mammal tree: species-level sets of phylogenies for questions in ecology, evolution, and conservation. *PLOS Biol.* (2019).

29. T. W. Davies, M. A. Bell, A. Goswami, T. J. D. Halliday, Completeness of the eutherian mammal fossil record and implications for reconstructing mammal evolution through the Cretaceous/Paleogene mass extinction. *Paleobiology* (2017), , doi:10.1017/pab.2017.20.

30. J. Alroy, M. D. Uhen, P. D. Mannion, C. Jaramillo, M. T. Carrano, L. W. van den Hoek Ostende, Taxonomic occurrences of Mammalia recorded in Fossilworks, the Evolution of Terrestrial Ecosystems database, and the Paleobiology Database. Fossilworks. http://fossilworks.org. (2018).

31. C. V. Bennett, P. Upchurch, F. J. Goin, A. Goswami, Deep time diversity of metatherian mammals: implications for evolutionary history and fossil-record quality. *Paleobiology*. **44**, 171–198 (2018).

32. R. W. Meredith, J. E. Janečka, J. Gatesy, O. A. Ryder, C. A. Fisher, E. C. Teeling, A. Goodbla, E. Eizirik, T. L. L. Simão, T. Stadler, D. L. Rabosky, R. L. Honeycutt, J. J. Flynn, C. M. Ingram, C. Steiner, T. L. Williams, T. J. Robinson, A. Burk-Herrick, M. Westerman, N. A. Ayoub, M. S. Springer, W. J. Murphy, Impacts of the Cretaceous Terrestrial Revolution and KPg Extinction on Mammal Diversification. *Science.* **334**, 521–524 (2011).

33. O. R. P. Bininda-Emonds, M. Cardillo, K. E. Jones, R. D. E. MacPhee, R. M. D. Beck, R. Grenyer, S. A. Price, R. A. Vos, J. L. Gittleman, A. Purvis, The delayed rise of present-day mammals. *Nature.* **446**, 507–512 (2007).

34. T. Stadler, Mammalian phylogeny reveals recent diversification rate shifts. *Proc. Natl. Acad. Sci.* **108**, 6187–6192 (2011).

35. S. A. Price, S. B. Hopkins, K. K. Smith, V. L. Roth, Tempo of trophic evolution and its impact on mammalian diversification. *Proc. Natl. Acad. Sci. USA*. **109**, 7008–7012 (2012).

36. J. Rolland, F. L. Condamine, F. Jiguet, H. Morlon, Faster Speciation and Reduced Extinction in the Tropics Contribute to the Mammalian Latitudinal Diversity Gradient. *PLOS Biol.* **12**, e1001775 (2014).

37. T. S. Kuhn, A. Ø. Mooers, G. H. Thomas, A simple polytomy resolver for dated phylogenies. *Methods Ecol. Evol.* **2**, 427–436 (2011).

38. S. Faurby, J.-C. Svenning, A species-level phylogeny of all extant and late Quaternary extinct mammals using a novel heuristic-hierarchical Bayesian approach. *Mol. Phylogenet. Evol.* **84**, 14–26 (2015).

39. E. Mayr, *Animal species and evolution* (Belknap, Cambridge, MA, 1963).

40. Y. Kisel, T. G. Barraclough, Speciation Has a Spatial Scale That Depends on Levels of Gene Flow. *Am. Nat.* **175**, 316–334 (2010).

41. S. Whitmee, C. D. L. Orme, Predicting dispersal distance in mammals: a trait-based approach. *J. Anim. Ecol.* **82**, 211–221 (2013).

42. Belliure, Sorci, Møller, Clobert, Dispersal distances predict subspecies richness in birds. *J. Evol. Biol.* **13**, 480–487 (2000).

43. S. Claramunt, E. P. Derryberry, J. V. Remsen, R. T. Brumfield, High dispersal ability inhibits speciation in a continental radiation of passerine birds. *Proc. R. Soc. Lond. B Biol. Sci.* **279**, 1567–1574 (2012).

44. E. B. Rosenblum, B. A. J. Sarver, J. W. Brown, S. D. Roches, K. M. Hardwick, T. D. Hether, J. M. Eastman, M. W. Pennell, L. J. Harmon, Goldilocks Meets Santa Rosalia: An Ephemeral Speciation Model Explains Patterns of Diversification Across Time Scales. *Evol. Biol.* **39**, 255–261 (2012).

45. D. Schluter, M. W. Pennell, Speciation gradients and the distribution of biodiversity. *Nature.* **546**, 48–55 (2017).

46. Soria-Carrasco Víctor, Castresana Jose, Diversification rates and the latitudinal gradient of diversity in mammals. *Proc. R. Soc. B Biol. Sci.* **279**, 4148–4155 (2012).

47. C. A. Botero, R. Dor, C. M. McCain, R. J. Safran, Environmental harshness is positively correlated with intraspecific divergence in mammals and birds. *Mol. Ecol.* **23**, 259–268 (2014).

48. M. P. Gerkema, W. I. L. Davies, R. G. Foster, M. Menaker, R. A. Hut, The nocturnal bottleneck and the evolution of activity patterns in mammals. *Proc R Soc B*. **280**, 20130508 (2013).

49. R. Maor, T. Dayan, H. Ferguson-Gow, K. E. Jones, Temporal niche expansion in mammals from a nocturnal ancestor after dinosaur extinction. *Nat. Ecol. Evol.* **1**, 1889 (2017).

50. J. H. Arbour, S. E. Santana, A major shift in diversification rate helps explain macroevolutionary patterns in primate species diversity. *Evolution.* **71**, 1600–1613 (2017).

51. J. D. Archibald, D. H. Deutschman, Quantitative Analysis of the Timing of the Origin and Diversification of Extant Placental Orders. *J. Mamm. Evol.* **8**, 107–124 (2001).

52. M. dos Reis, J. Inoue, M. Hasegawa, R. J. Asher, P. C. J. Donoghue, Z. Yang, Phylogenomic datasets provide both precision and accuracy in estimating the timescale of placental mammal phylogeny. *Proc. R. Soc. Lond. B Biol. Sci.* **279**, 3491–3500 (2012).

53. M. M. Pires, B. D. Rankin, D. Silvestro, T. B. Quental, Diversification dynamics of mammalian clades during the K–Pg mass extinction. *Biol. Lett.* **14**, 20180458 (2018).

54. D. M. Grossnickle, E. Newham, Therian mammals experience an ecomorphological radiation during the Late Cretaceous and selective extinction at the K–Pg boundary. *Proc R Soc B*. **283**, 20160256 (2016).

55. D. M. Grossnickle, S. M. Smith, G. P. Wilson, Untangling the Multiple Ecological Radiations of Early Mammals. *Trends Ecol. Evol.* (2019), doi:10.1016/j.tree.2019.05.008.

56. D. L. Rabosky, Automatic detection of key innovations, rate shifts, and diversity-dependence on phylogenetic trees. *PLoS ONE*. **9**, e89543 (2014).

57. B. R. Moore, K. M. A. Chan, M. J. Donoghue, in *Phylogenetic Supertrees*, O. R. P. Bininda-Emonds, Ed. (Springer Netherlands, 2004; http://link.springer.com/chapter/10.1007/978-1-4020-2330-9_23), *Computational Biology*, pp. 487–533.

58. S. Nee, E. C. Holmes, R. M. May, P. H. Harvey, Extinction rates can be estimated from molecular phylogenies. *Philos. Trans. R. Soc. Lond. B-Biol. Sci.* **344**, 77–82 (1994).

59. J. J. Schenk, K. C. Rowe, S. J. Steppan, Ecological opportunity and incumbency in the diversification of repeated continental colonizations by muroid rodents. *Syst. Biol.* **62**, 837–864 (2013).

60. D. L. Rabosky, H. Huang, A Robust Semi-Parametric Test for Detecting Trait-Dependent Diversification. *Syst. Biol.* **65**, 181–193 (2016).

61. H. Morlon, T. L. Parsons, J. B. Plotkin, Reconciling molecular phylogenies with the fossil record. *Proc. Natl. Acad. Sci.* **108**, 16327–16332 (2011).

62. S. Louca, M. W. Pennell, Phylogenies of extant species are consistent with an infinite array of diversification histories. *bioRxiv*, 719435 (2019).

63. N. D. Pyenson, The Ecological Rise of Whales Chronicled by the Fossil Record. *Curr. Biol.* **27**, R558–R564 (2017).

64. J. J. Shi, D. L. Rabosky, Speciation dynamics during the global radiation of extant bats. *Evolution*. **69**, 1528–1545 (2015).

65. L. I. Amador, R. L. M. Arévalo, F. C. Almeida, S. A. Catalano, N. P. Giannini, Bat Systematics in the Light of Unconstrained Analyses of a Comprehensive Molecular Supermatrix. *J. Mamm. Evol.* **25**, 37–70 (2018).

66. W. Jetz, G. H. Thomas, J. B. Joy, K. Hartmann, A. O. Mooers, The global diversity of birds in space and time. *Nature*. **491**, 444–448 (2012).

67. S. Wright, The "Age and Area" Concept Extended. *Ecology*. **22**, 345–347 (1941).

68. G. G. Simpson, *The major features of evolution* (Columbia Univ Press, New York, 1953).

69. A. von Hardenberg, A. Gonzalez-Voyer, Disentangling Evolutionary Cause-Effect Relationships with Phylogenetic Confirmatory Path Analysis. *Evolution*. **67**, 378–387 (2013).

70. R. P. Freckleton, A. B. Phillimore, M. Pagel, Relating Traits to Diversification: A Simple Test. *Am. Nat.* **172**, 102–115 (2008).

71. D. Jablonski, Heritability at the Species Level: Analysis of Geographic Ranges of Cretaceous Mollusks. *Science*. **238**, 360–363 (1987).

72. D. L. Rabosky, P. O. Title, H. Huang, Minimal effects of latitude on present-day speciation rates in New World birds. *Proc R Soc B*. **282**, 20142889 (2015).

73. G. Hewitt, The genetic legacy of the Quaternary ice ages. *Nature*. **405**, 907–913 (2000).

74. J. D. Marcot, D. L. Fox, S. R. Niebuhr, Late Cenozoic onset of the latitudinal diversity gradient of North American mammals. *Proc. Natl. Acad. Sci.* **113**, 7189–7194 (2016).

75. J. B. Yoder, E. Clancey, S. Des Roches, J. M. Eastman, L. Gentry, W. Godsoe, T. J. Hagey, D. Jochimsen, B. P. Oswald, J. Robertson, B. A. J. Sarver, J. J. Schenk, S. F. Spear, L. J. Harmon, Ecological opportunity and the origin of adaptive radiations. *J. Evol. Biol.* **23**, 1581–1596 (2010).

76. H. Wilman, J. Belmaker, J. Simpson, C. de la Rosa, M. M. Rivadeneira, W. Jetz, EltonTraits 1.0: Species-level foraging attributes of the world's birds and mammals. *Ecology*. **95**, 2027–2027 (2014).

591 77. K. E. Jones, J. Bielby, M. Cardillo, S. A. Fritz, J. O'Dell, C. D. L. Orme, K. Safi, W.
592   Sechrest, E. H. Boakes, C. Carbone, C. Connolly, M. J. Cutts, J. K. Foster, R. Grenyer, M.
593   Habib, C. A. Plaster, S. A. Price, E. A. Rigby, J. Rist, A. Teacher, O. R. P. Bininda-
594   Emonds, J. L. Gittleman, G. M. Mace, A. Purvis, PanTHERIA: a species-level database of
595   life history, ecology, and geography of extant and recently extinct mammals. *Ecology*. **90**,
596   2648–2648 (2009).
597 78. M. Steel, A. Mooers, The expected length of pendant and interior edges of a Yule tree. *Appl.*
598   *Math. Lett.* **23**, 1315–1319 (2010).
599 79. I. Quintero, W. Jetz, Global elevational diversity and diversification of birds. *Nature* (2018).
600 80. P. O. Title, D. L. Rabosky, Tip rates, phylogenies and diversification: What are we
601   estimating, and how good are the estimates? *Methods Ecol. Evol.* **10**, 821–834 (2019).
602 81. M. R. May, S. Höhna, B. R. Moore, A Bayesian approach for detecting the impact of mass-
603   extinction events on molecular phylogenies when rates of lineage diversification may vary.
604   *Methods Ecol. Evol.* **7**, 947–959 (2016).
605 82. J. Alroy, Accurate and precise estimates of origination and extinction rates. *Paleobiology*.
606   **40**, 374–397 (2014).
607 83. M. Foote, Origination and extinction components of taxonomic diversity: general problems.
608   *Paleobiology*. **26**, 74–102 (2000).
609 84. L. J. Revell, phytools: an R package for phylogenetic comparative biology (and other things).
610   *Methods Ecol. Evol.* **3**, 217–223 (2012).
611 85. D. L. Rabosky, Likelihood methods for detecting temporal shifts in diversification rates.
612   *Evolution*. **60**, 1152–1164 (2006).
613 86. L. S. T. Ho, C. Ané, A Linear-Time Algorithm for Gaussian and Non-Gaussian Trait
614   Evolution Models. *Syst. Biol.* **63**, 397–408 (2014).
615 87. M. G. Harvey, G. F. Seeholzer, B. T. Smith, D. L. Rabosky, A. M. Cuervo, R. T. Brumfield,
616   Positive association between population genetic differentiation and speciation rates in New
617   World birds. *Proc. Natl. Acad. Sci.* **114**, 6328–6333 (2017).
618 88. W. van der Bijl, phylopath: Easy phylogenetic path analysis in R. *PeerJ*. **6**, e4718 (2018).
619

620 **Figure legends**

621 **Fig. 1. Species-level relationships, rates, and traits for 5,911 species of mammals globally.**

622 (**a**) The maximum clade credibility topology of 10,000 node-dated trees, with numbered clade

623 labels corresponding to orders and subclades listed in the plot periphery: Eulipoty., Eulipotyphla;

624 Carn., Carnivora; Artio., Artiodactyla. Scale in millions of years, Ma. Branches are colored with

625 tip-level speciation rates (tip DR metric) and marked with 24 inferred shifts in branch-specific

626 net diversification rates (nodes A-X; shifts with multiple circles occurred on either branch, not

627 both). Tip-level rates are reconstructed to interior branches using Brownian motion. (**b**) Per-

628 species ecological traits: allometric index of vagility (dispersal ability), diurnality (predominant

629 daytime activity), and north-south latitudinal extent (see *Methods* for details). Silhouettes are

630 from phylopic.org and open source fonts.

631 **Fig. 2. Diversification rate variation among mammal clades.** Lineage-through-time plots and

632 estimated crown ages for (**a**) all superordinal divergences (y-axis does not apply to error bars),

633 and (**b**) placental orders with crown age estimates overlapping the Cretaceous-Paleogene

634 extinction event (K-Pg, dashed gray line; means and 95% CIs; filled circle if statistically

635 different). (**c**) Rate-through-time plots for speciation, extinction, and net diversification

636 (summarized from Fig. 1 rate shifts; medians from 10 trees, 95% CIs in light gray). (**d**) Fossil

637 genus diversity through time for all Mammalia, including subsampled genus richness (quorum

638 0.5) and per-capita rates of genus origination and extinction. (**e**) Extant rates and lineage-specific

639 rate shifts for the five most speciose mammal orders (same symbols as in **c**). (**f**) Rate variation

640 within subclades of these five orders as numbered from Fig. 1; left: difference in AIC between

641 best-fit models of diversification for trees simulated under rate-constant birth-death (gray) versus

642 observed mammal trees (color; filled circle and * if ΔAIC on 100 trees is statistically different);

643 and, right: tip-level speciation rate (tip DR metric) distributions of the same simulated and

644 observed subclades (gray versus color, one tree), comparing variation in clade tip rate mean and

645 skew across 100 trees. The last 2 Ma are removed from parts **c-e** to focus on pre-recent rate

646 dynamics.

647 **Fig. 3. Explanation of time-sliced clade delimitation and summarization for testing**
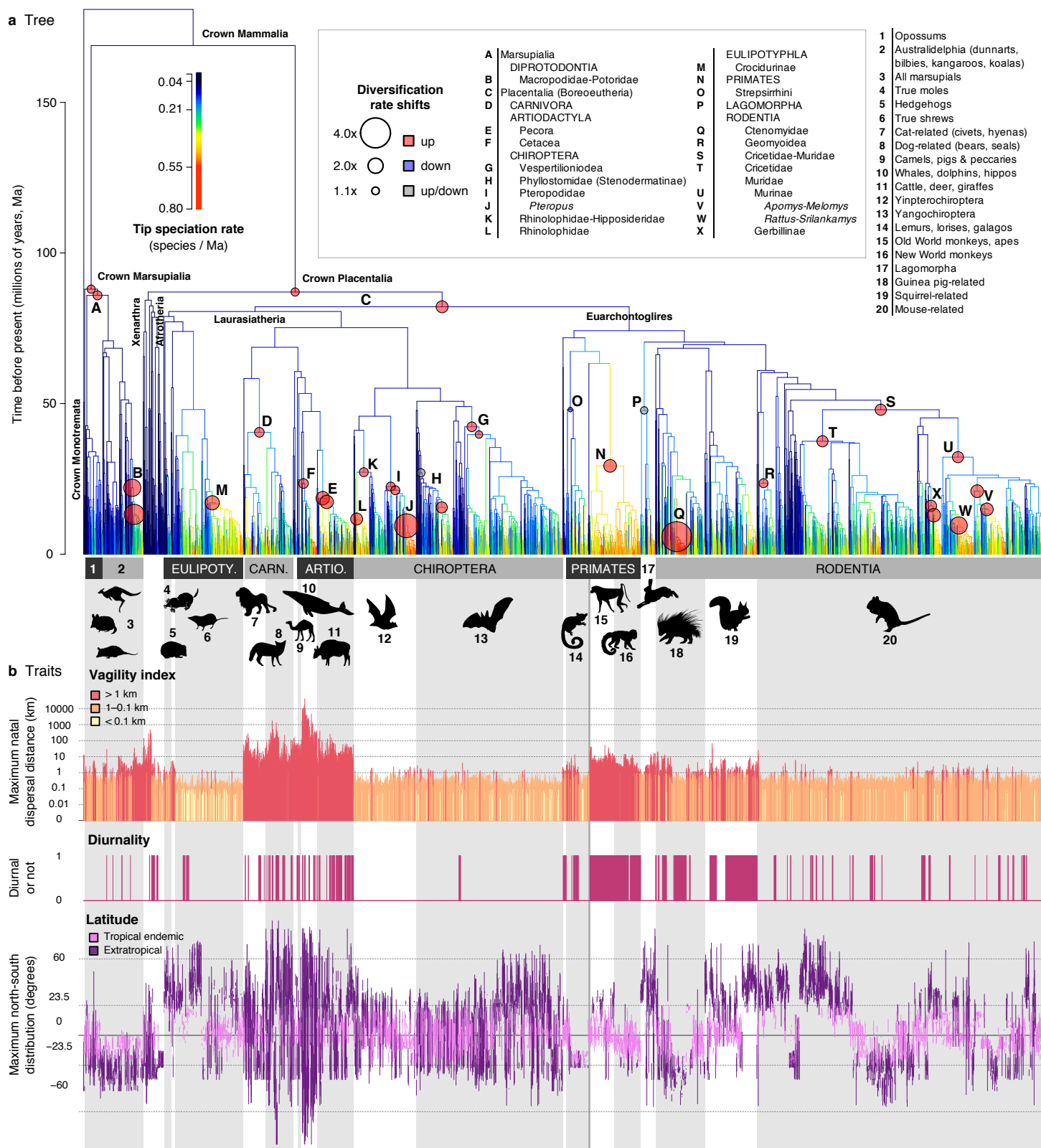
648 **hypotheses.** (**a and b**) An example subclade of 64 species, the rodent family Heteromyidae, is

649 divided into time-sliced clades in the same way as for all Mammalia. Branch colors in the

20

650   family-level phylogeny correspond to tip-level diversification rates (tip DR) calculated on the

651   full tree, and red symbols are sized according to estimates of species vagility. An example time

652   slice for 5-Ma tipward clades is shown with summaries of tip DR mean and vagility (harmonic

653   and geometric means) to compare to clade crown age and richness. (**c**) Example Mammalia-wide

654   time slice at 35 Ma delimiting clades for multivariate PGLS (phylogenetic generalized least

655   squares) analysis on log clade richness, as was performed on 100 trees throughout this study.

656   Observed mammal clades are compared to clades from simulated rate-constant trees of the same

657   age and richness. (**d**) Results for clades defined at time-slices every 5 Ma for log clade richness

658   and its variance, as compared among empirical mammal trees and simulated trees.

659   **Fig. 4. Age and rate components of species richness variation across time-slice defined**

660   **clades.** (**a**) The log species richness of clades tipward of each 5-Ma time slice (dotted lines from

661   5-70 Ma) across a sample of 100 phylogenies (maximum clade credibility tree shown) is best

662   predicted jointly by clade crown age, (**b**) clade tip DR mean, and (**c**) clade tip DR skew.

663   Multivariate phylogenetic analyses of clade richness in observed trees (grey) is compared to trees

664   simulated under rate-constant birth and death with different extinction fractions, ε (colours in

665   legend; PGLS on standardized data with 95% confidence intervals [CIs] on parameter estimates).

666   Solid black lines are the observed best-fitting models given random effects of time slice and tree.

667   **Fig. 5. Connecting clade ages, rates, richness, and traits in the mammal tree of life.** (**a**, top

668   panel) Distribution of tip-level speciation rates (tip DR metric, harmonic mean of 10,000 trees)

669   relative to per-species estimates of vagility (maximum natal dispersal distance), diurnality

670   (0=nocturnal or cathemeral, 1=diurnal), and absolute value of latitude (centroid of expert maps)

671   across 5,675 species (excluding extinct and marine species). Loess smoothing lines visualize

672   general trends (blue, span=0.33). Tip-level effects (bottom panel) from univariate PGLS between

673   tip speciation rates and ecological traits subset across trophic levels (1000 trees, 95% CI, colored

674   if significant). (**b**) Phylogenetic path analysis (*69*) of putative causal relationships between traits

675   and rates leading to clade species richness for time-sliced clades. Path thickness, color, and

676   directionality denote median coefficients of model-averaged analyses. The bottom panels provide

677   per-estimate uncertainty across time slices (slope ± SE, 1000 trees). Non-zero estimates, either

678   positive (blue shades) or negative (red shades), are totaled in the right margin; paths present in

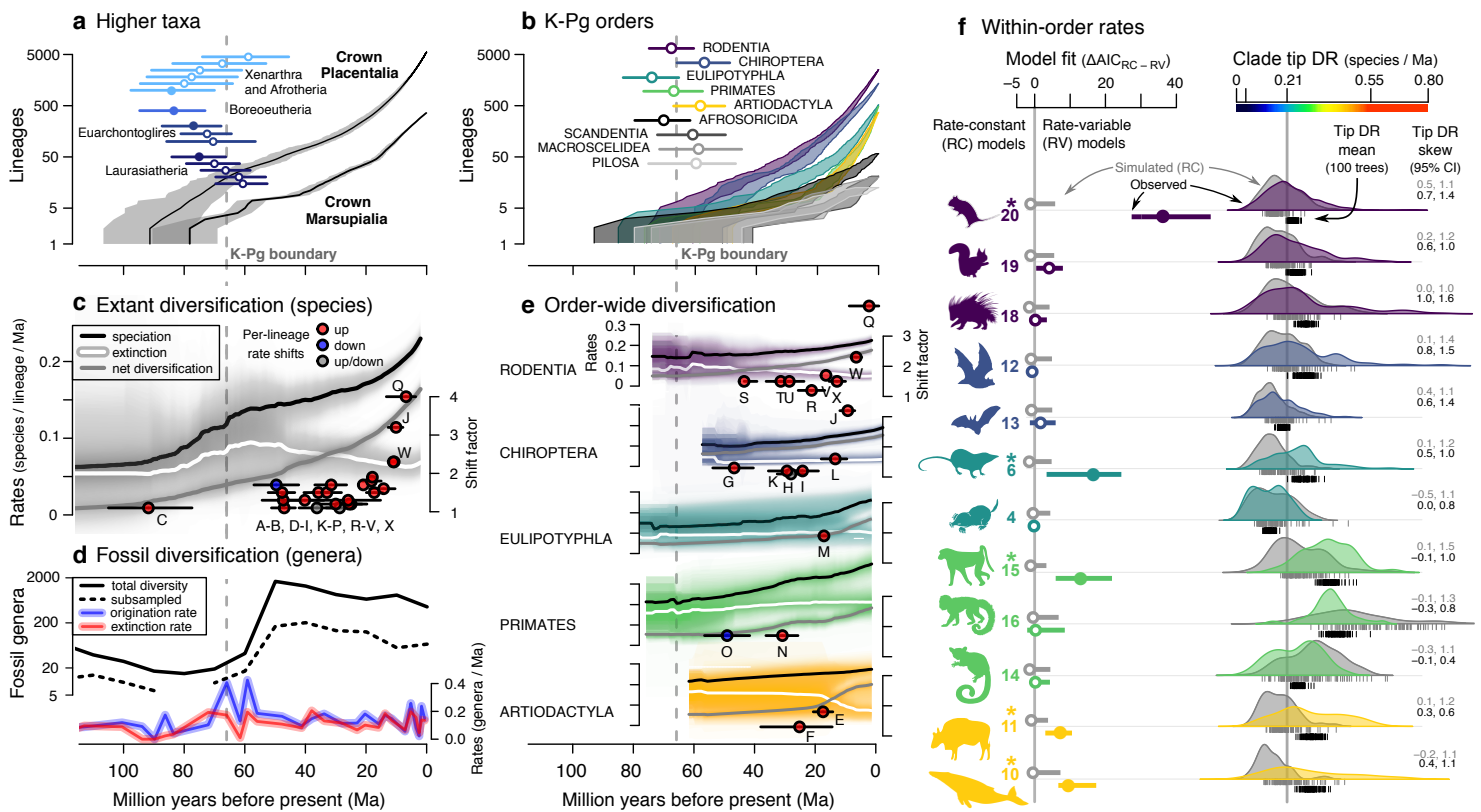679   >500 trees are bolded and displayed in path model whereas others are dashed.

21

Fig. 1. Species-level relationships, rates, and traits for 5,911 species of mammals globally. (a) The maximum clade credibility topology of 10,000 node-dated trees, with numbered clade labels corresponding to orders and subclades listed in the plot periphery: Eulipoty., Eulipotyphla; Carn., Carnivora; Artio., Artiodactyla. Scale in millions of years, Ma. Branches are colored with tip-level speciation rates (tip DR metric) and marked with 24 inferred shifts in branch-specific net diversification rates (nodes A-X; shifts with multiple circles occurred on either branch, not both). Tip-level rates are reconstructed to interior branches using Brownian motion. **(b)** Per-species ecological traits: allometric index of vagility (dispersal ability), diurnality (predominant daytime activity), and north-south latitudinal extent (see *Methods* for details). Silhouettes are from phylopic.org and open source fonts.

Fig. 2. Diversification rate variation among mammal clades. Lineage-through-time plots and estimated crown ages for (**a**) all superordinal divergences (y-axis does not apply to error bars), and (**b**) placental orders with crown age estimates overlapping the Cretaceous-Paleogene extinction event (K-Pg, dashed grey line; means and 95% CIs; filled circle if statistically different). (**c**) Extant rates of speciation, extinction, and net diversification through time on the full Mammalia phylogeny relative to lineage-specific shifts in net diversification (median rates from 10 trees, 95% CIs in light grey). (**d**) Fossil genus diversity through time for all Mammalia, including subsampled genus richness (quorum 0.5) and per-capita rates of genus origination and extinction. (**e**) Extant rates and lineage-specific rate shifts for the five most speciose mammal orders (same symbols as in **c**). (**f**) Rate variation within subclades of these five orders (numbers correspond to Fig. 1); left: quantified as difference in AIC between best-fit models of diversification (ΔAIC_{RC-RV} median and 95% CIs on 100 trees) for trees simulated under rate-constant birth-death (RC, grey) versus observed mammal trees (colour; * and filled circle if statistically different); and, right: example tip DR distributions of the same simulated and observed subclades (grey versus colour, one tree), comparing variation in tip DR mean and skew relative to the median for all Mammalia (grey line, 100 trees). The last 2 Ma are removed from parts **c-e** to focus on pre-recent rate dynamics.
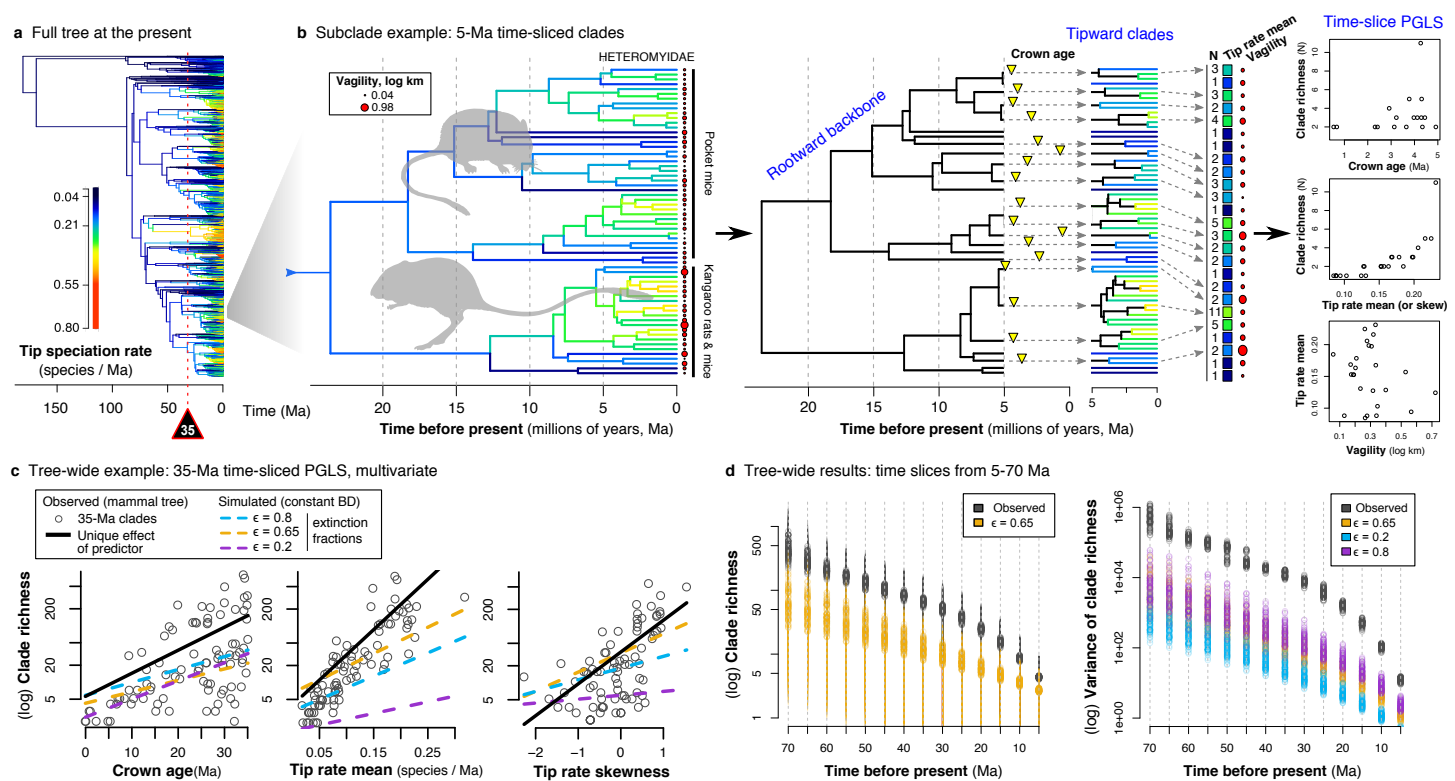
Fig. 3. Explanation of time-sliced clade delimitation and summarization for testing hypotheses. (a and b) An example subclade of 64 species, the rodent family Heteromyidae, is divided into time-sliced clades in the same way as for all Mammalia. Branch colors in the family-level phylogeny correspond to tip-level diversification rates (tip DR) calculated on the full tree, and red symbols are sized according to estimates of species vagility. An example time slice for 5-Ma tipward clades is shown with summaries of tip DR mean and vagility (harmonic and geometric means) to compare to clade crown age and richness. **(c)** Example Mammalia-wide time slice at 35 Ma delimiting clades for multivariate PGLS (phylogenetic generalized least squares) analysis on log clade richness, as was performed on 100 trees throughout this study. Observed mammal clades are compared to clades from simulated rate-constant trees of the same age and richness. **(d)** Results for log clade richness and its variance comparing clades defined at time-slices every 5 Ma for observed mammal trees (grey) and trees simulated with different extinction fractions (ε, colored).
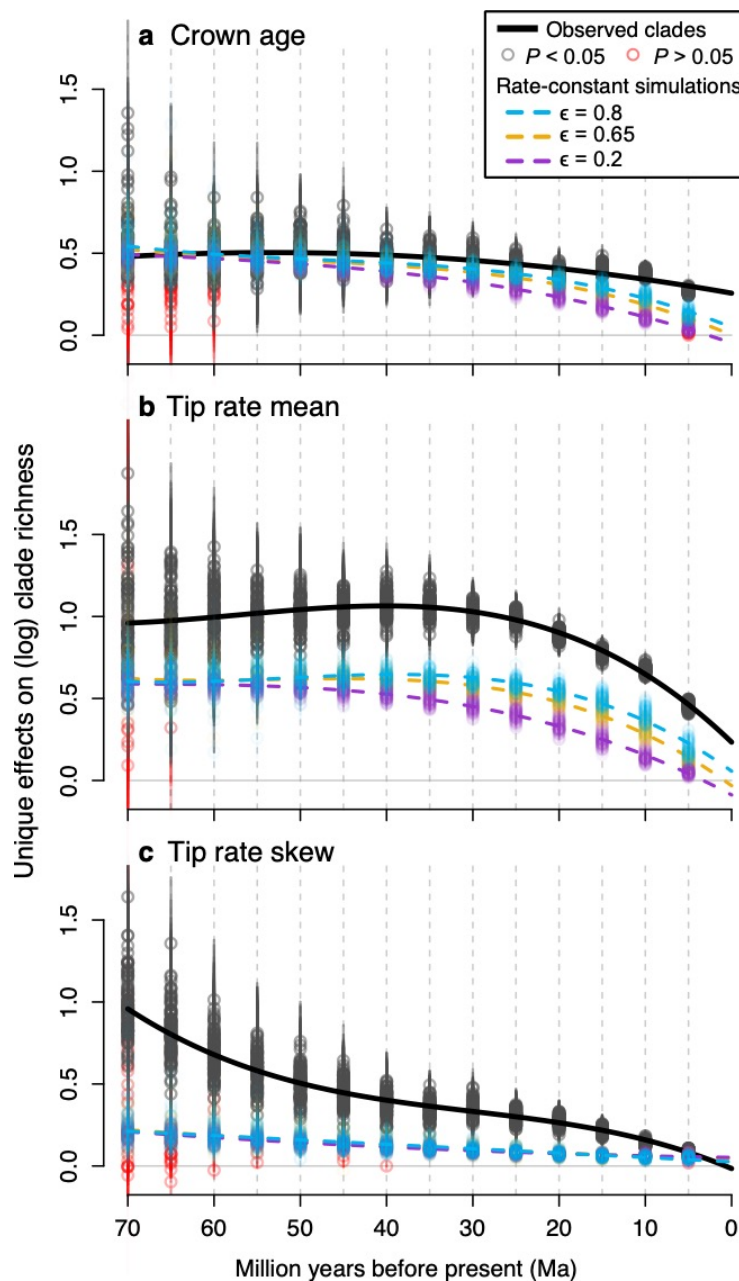
Fig. 4. Age and rate components of species richness variation across time-slice defined clades. (a) The log species richness of clades tipward of each 5-Ma time slice (dotted lines from 5-70 Ma) across a sample of 100 phylogenies (maximum clade credibility tree shown) is best predicted jointly by clade crown age, (b) clade tip DR mean, and (c) clade tip DR skew. Multivariate phylogenetic analyses of clade richness in observed trees (grey) is compared to trees simulated under rate-constant birth and death with different extinction fractions, ε (colours in legend; PGLS on standardized data with 95% confidence intervals [CIs] on parameter estimates). Solid black lines are the observed best-fitting models given random effects of time slice and tree.
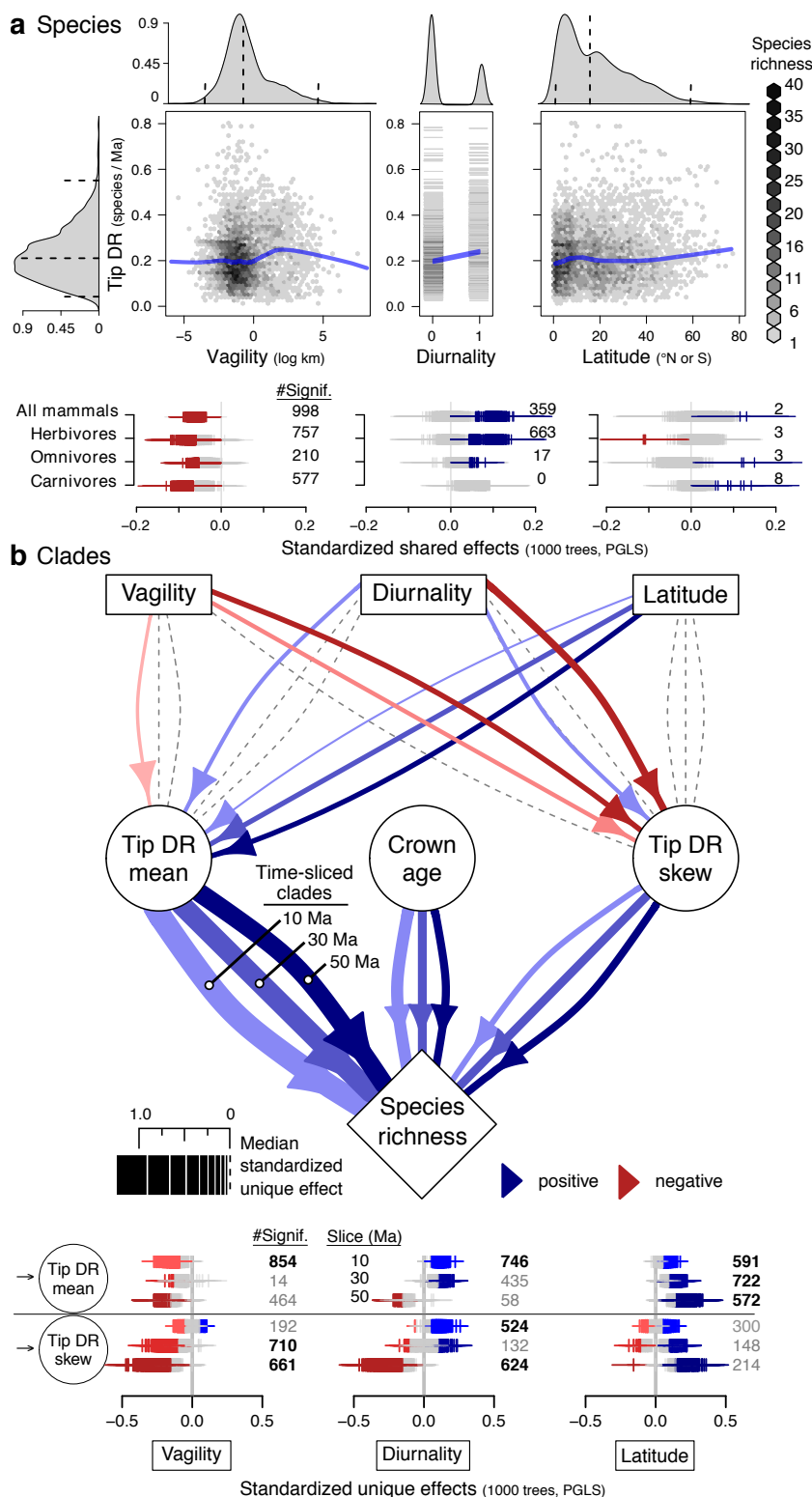
Fig. 5. Connecting clade ages, rates, richness, and traits in the mammal tree of life. (**a**, top panel) Distribution of species-level diversification rates (tip DR, mean of 10,000 trees) relative to per-species estimates of vagility (maximum natal dispersal distance), diurnality (0=nocturnal, 1=diurnal or cathemeral), and absolute value of latitude (centroid of expert range maps) across 5,675 species (excluding extinct and marine species). Loess smoothing lines visualize general trends (blue, span=0.33). Species-level effects (bottom panel) from univariate PGLS between tip DR and ecological traits subset across trophic categories (1000 trees, 95% CI, coloured if significant). (**b**) Phylogenetic path analysis of putative causal relationships between traits and rate-based processes leading to clade species richness for time-sliced clades. Path thickness, colour, and directionality denote median coefficients of model-averaged analyses. The bottom panels provide per-estimate uncertainty across analyses and time slices (slope ± SE, 1000 trees). Non-zero estimates, either positive (blue shades) or negative (red shades), are totalled in the right margin; paths present in >500 trees are bolded and displayed in path model whereas other paths have dashed lines.